Microwave-activated CuO nanotip/ZnO nanorod nanoarchitectures for efficient hydrogen production†

Yan-Gu Lin,[a] Yu-Kuei Hsu,[b] San-Yuan Chen,[a] Li-Chyong Chen*[c] and Kuei-Hsien Chen*[bc]

Received 9th September 2010, Accepted 4th November 2010
DOI: 10.1039/c0jm03022h

Microwave treatment of CuO nanotip/ZnO nanorod catalyst precursors has been demonstrated to remarkably enhance their activity in methanol reforming reactions. Studies using XRD, Raman, XPS, XAS, and HRTEM analyses conclude that comparative to conventional heating, microwave treatment significantly enhances the activity and stability of the catalysts, which might be attributed to defect and microstrain formation and strong metal support interaction at the Cu/ZnO interface.

In the field of development of advanced energy-related devices, nanostructured materials have attracted great interest in recent years due to their intriguing physical and chemical properties that are significantly different from their bulk counterparts.[1] Nanostructured catalysts are expected to be the key components in the advancement of future energy technologies. Hence, new strategies for the synthesis of high-performance nanomaterials are widely pursued.[2] In particular, Cu/ZnO-based catalysts have been extensively investigated because of their importance in several industrial applications, such as methanol synthesis, CO removal, and hydrogen generation.[3,4] Nanostructured catalysts consisting of microporous structures are attractive for flow-type gas-solid reactions due to their effective diffusion of reactants and heat. In our previous work, a strong metal-support interaction (SMSI) effect in arrayed ZnO NR@Cu nanoparticle (NP) nanocomposites was shown to cause microstrain in the Cu NPs, to which an increase in catalytic performance was attributed.[5] These findings led us to design and develop a very effective technique to tailor the Cu/ZnO interface.

In recent years, microwave (MW) irradiation has become an effective tool in synthetic organic chemistry, yielding dramatic increases in reaction rates and yields.[6] Moreover, since the magnitude of MW absorption is related to dipole oscillation in a material, MW annealing can provide selective heating and lead to a new route for material processing. Recently, application of MW as selective annealing technique has attracted tremendous attention for improving the efficiency of polymer organic photovoltaic devices.[7] In this communication, we report MW treatment of nanoarchitectures of CuO nanotips (NTs) on ZnO nanorod (NR) frameworks as catalyst precursors for methanol reforming reactions (MRRs).

Our initial attempts employing a surfactant-free approach (ammonia-evaporation-induced synthetic method) for the synthesis of CuO nanostructures[8] resulted in the formation of radiating nanosheets as shown in Fig. 1a. The high-resolution transmission electron microscopy (HRTEM) image in Fig. S1 (ESI†) provides specific structural information about an individual nanosheet grown along the [11$\bar{1}$] direction. Interestingly, while ZnO NRs were introduced as scaffolds for the heterogeneous nucleation and growth of CuO, different morphologies of CuO were observed, ranging from nanosheets to NTs (Fig. 1b). Fig. S2 (ESI†) presents the TEM and HRTEM images of CuO NT/ZnO NR catalyst precusors synthesized in this work, showing that NTs not only adhere to but also directly conjoin with the NR. While detailed understanding of the growth mechanism is essential, the nanoarchitecture provides opportunity for advanced applications such as nano-catalysis.

In order to gain an insight into the changes in microstructure, electronic configuration, and reducibility of various CuO NT/ZnO NR catalyst precusors, X-ray diffraction (XRD), X-ray photoelectron spectroscopy (XPS), X-ray absorption spectroscopy (XAS), N_2O titration, micro-Raman spectroscopy, and temperature-programmed reduction (TPR) investigations were performed. Fig. 2a presents the XRD patterns of CuO NT/ZnO NR catalyst precusors after MW irradiation and conventional thermal annealing. Noticeable shifts in the CuO diffraction peaks are observed, especially after MW irradiation. This is due, presumably, to CuO being partially dissolved in the ZnO lattice, leading to the creation of microstrain between NTs and NRs. Moreover, the CuO(111) peak shows a significant up-shift after MW irradiation, implying that a specific MW treatment can enhance the degree of microstructural disorder in CuO NTs. In contrast, there is no remarkable change in the position of CuO(111) peak of NT/NR nanocomposites after conventional thermal annealing. The above observations are well complemented by the micro-Raman results presented in Fig. 2b, in which a main peak at around 438 cm^{-1} corresponding to the characteristic E_2(high) vibrational mode of ZnO, and another major peak at about 286 cm^{-1} (A_g mode) attributed to the vibrations of oxygen atoms in CuO were

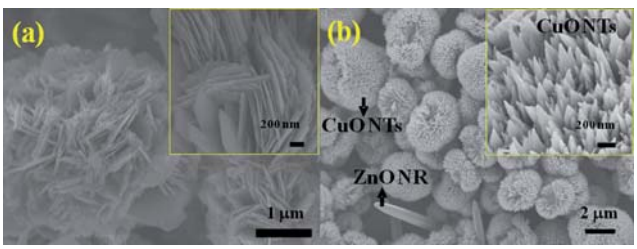

Fig. 1 (a) SEM images of CuO nanostructures (inset: high magnification). (b) SEM images of CuO NT/ZnO NR catalyst precusors (inset: high magnification).

[a]*Department of Materials Science and Engineering, National Chiao Tung University, Hsinchu, 30010, Taiwan*
[b]*Institute of Atomic and Molecular Sciences, Academia Sinica, Taipei, 10617, Taiwan. E-mail: chenkh@pub.iams.sinica.edu.tw; Fax: +886-2-2362-0200; Tel: +886-2-2366-8232*
[c]*Center for Condensed Matter Sciences, National Taiwan University, Taipei, 10617, Taiwan. E-mail: chenlc@ntu.edu.tw*

† Electronic supplementary information (ESI) available: Experimental details of the synthesis and characterization (TEM and HRTEM images). See DOI: 10.1039/c0jm03022h

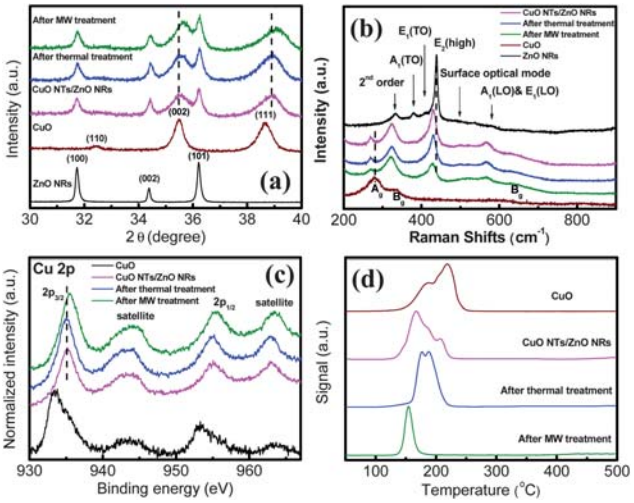

Fig. 2 (a) X-Ray diffraction, (b) micro-Raman, (c) X-ray photo-electron spectroscopy, and (d) TPR spectra of the as-prepared, after thermal treatment, and after MW treatment CuO NT/ZnO NR catalyst precursors.

observed.[9] Significant variations in peak position as well as full width at half maximum (FWHM) of both E_2(high) and A_g modes occur as a result of the formation of CuO/ZnO nanoarchitectures. These variations are believed to be strongly related to the strain-induced shift and broadening of the phonon modes. Moreover, higher FWHMs of E_2(high) and A_g modes after MW treatment suggest a significant change in band structure of NT/NR nanoarchitectures, indicating that specific MW treatment can enhance the magnitude of lattice distortions. Further evidence is obtained by HRTEM observations (presented in Fig. S3, ESI†), that clearly shows a highly distorted lattice as a result of MW irradiation.

Fig. 2c presents the Cu 2p core level XPS spectra of NR-NT catalyst precursors after MW irradiation and conventional thermal annealing. The position of the main peak, corresponding to Cu $2p_{3/2}$ transition, shifts to higher binding energy for CuO/ZnO catalyst precursors. This clearly indicates a modification of the electron density on CuO species due to the interactive coupling between CuO and ZnO. Furthermore, unlike that for the conventional thermal annealing, the position of the main Cu $2p_{3/2}$ peak continues to up-shift after MW irradiation. This up-shift results from further distortions of the CuO lattice due to the presence of microstrain between NTs and NRs. This behavior agrees well with the XRD and micro-Raman results discussed above. TPR analysis was also carried out to determine the reducibility of surface oxygen in CuO/ZnO catalyst precursors presented in Fig. 2d. In contrast to pure CuO, the CuO NT/ZnO NR catalyst precursors apparently lower the reduction temperature of CuO. This is probably due to weakening of the Cu–O bond due to the presence of strongly bound ZnO species. More surprisingly, CuO NT-immobilized ZnO NR catalyst precursors exhibit a notable shift in the reduction peak to the lowest temperature after MW irradiation, as compared to the conventional thermal annealing. Furthermore, a narrower TPR peak is observed in the MW-treated CuO NT/ZnO NR sample. They indicate far superior redox properties for CuO NT/ZnO NR catalyst precursors, due to the SMSI effect caused by MW irradiation.

Fig. 3a and 3b compare the effects of MW and conventional thermal treatments on the methanol conversion as well as hydrogen production rates. After H_2 pre-reduction of CuO NT/ZnO NR

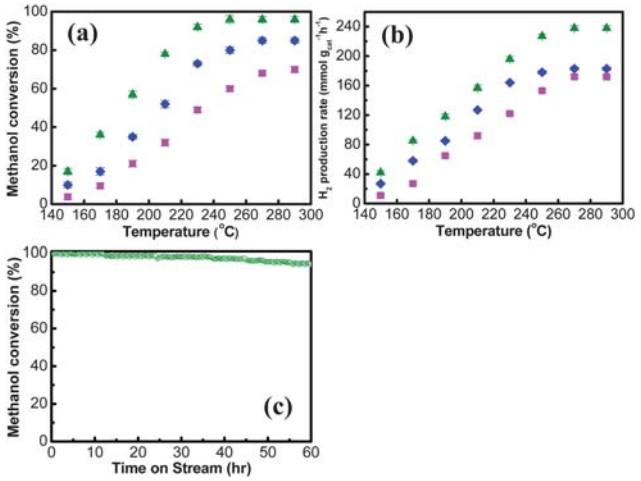

Fig. 3 Methanol reforming reaction profiles: (a) methanol conversion rate and (b) hydrogen production rate for Cu NTs/ZnO NR working catalysts: as-prepared (■), after thermal treatment (◆), and after MW treatment (▲). Reaction conditions: $H_2O : O_2 : MeOH = 1 : 0.125 : 1$, $W/F = 21\ kg_{cat}\ s\ mol^{-1}_{methanol}$. (c) Stability test in a MRR over MW-treated Cu NT/ZnO NR working catalysts at $H_2O : O_2 : MeOH = 1 : 0.125 : 1$, $T = 250\ °C$, and $W/F = 21\ kg_{cat}\ s\ mol^{-1}_{methanol}$.

catalyst precursors, all experiments were run for 12 h with a working catalyst (Cu NT/ZnO NR). The chemical state of Cu could be determined *via* X-ray absorption near-edge spectroscopy (XANES) measurements (Fig. 4a), showing all the CuO will turn to metallic Cu (serving as the active species for MRRs). Meanwhile, most experiments were repeated for several catalysts. No significant deactivation of catalysts was noted in these experiments. In addition, the structural factor such as morphology and Cu surface area, which would generally affect the activity of Cu-based catalysts for MRRs, have been completely excluded *via* N_2O titration measurement, showing no remarkable change of Cu surface area (about 45.7 $m^2\ g^{-1}$) with or without MW irradiation and conventional thermal annealing. The methanol conversion and hydrogen production rates over the pristine Cu/ZnO working catalysts were close to 70% and 170 mmol $g_{cat}^{-1}\ h^{-1}$ at 290 °C, respectively. Interestingly, after MW irradiation, the methanol conversion and hydrogen production rates increased to 96% and 230 mmol $g_{cat}^{-1}\ h^{-1}$ (at only 250 °C) respectively, which are significantly higher than those obtained by the conventional thermal annealing of the NT/NR catalysts. Furthermore, the amounts of CO produced in the gas outlet is another indication of the activity. The

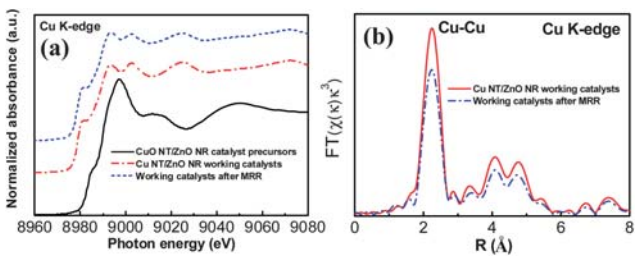

Fig. 4 (a) Cu K-edge XANES and (b) Cu K-edge EXAFS of CuO NT/ZnO NR catalyst precursors with MW irradiation, MW-treated Cu NT/ZnO NR working catalysts, and MW-treated Cu NT/ZnO NR working catalysts after continuously operating for 60 h in a MRR.

CO concentration of only 170–210 ppm at 250 °C produced from the MW-treated Cu NT/ZnO NR catalyst is substantially lower that the typically 300 ppm CO produced from a conventional thermal annealed samples. Therefore, the new catalyst developed here represents a promising candidate for use in catalytic generation of high purity hydrogen for fuel cell applications.

Previous investigations pertaining to heat treatment of the catalytic materials using MW irradiation also revealed selective heating of specific catalytic sites and led to "molecular hot spots" in the catalysts.[10] For the binary system comprising CuO/ZnO catalyst precursors, only the CuO component is known to be a strong MW absorber.[11] Therefore, hot spot formation at CuO sites decorated on the ZnO support is likely to result in pronounced microstructural rearrangement at the NT/NR interface due to selective MW absorption by CuO. This may account for the good correlation between the increase in defects in NTs and the enhancement in catalytic performance after MW treatment. In this respect, MW processing of the hybrid CuO NT/ZnO NR catalyst precursors appears to provide a unique opportunity for generating significant microstructural deformation at the NT/NR interface due to the formation of hot spots as a consequence of selective dielectric heating, thus leading to the desired creation of highly strained CuO NTs. Last but not least, the advantage of MW-treated NT/NR working catalysts is further exemplified by the excellent stability (only 6% reduction after 60 h of operation) in MRRs as shown in Fig. 3c. The reason is the chemical state of metallic Cu (serving as the active species) could be maintained after long-term operation in MRRs as shown in Fig. 4a. This is significantly enhanced comparative to the 11.5% and 33.8% reduction after 36 h operation for other catalysts without MW-treatment reported earlier.[5] The slight decay of methanol conversion may be due to the decrease of crystallinity in Cu lattice after continuous 60 h operation (Fig. 4b). From extended X-ray absorption fine structure (EXAFS) analyses as shown in Fig. 4b, an apparent decrease in the intensity of the first-shell (Cu–Cu bonding) over MW-treated Cu NT/ZnO NR working catalysts after long-term operation in MRRs could be observed.

In summary, we have demonstrated an effective MW-treatment technique to enhance the catalytic activity of CuO NT/ZnO NR nanostructures for the MRR. Not only higher conversion efficiency and lower operation temperature, but also lower CO production and remarkably enhanced stability of the MW-treated catalysts have been achieved. It's believed that formation of defects, microstrains and SMSI due to the selective heating by MW-treatment may have contributed to such enhancement in catalyst performance. This finding offers an alternative route using MW-treatment to enhance the activity of a wide range of catalysts.

Acknowledgements

This work was supported by the National Natural Science Council, Ministry of Education, Taiwan, and AOARD under AFSOR, US.

Notes and references

1 M. Law, L. E. Greene, J. C. Johnson, R. Saykally and P. Yang, *Nat. Mater.*, 2005, **4**, 455; R. Si and M. Flytzani-Stephanopoulos, *Angew. Chem., Int. Ed.*, 2008, **47**, 2884; Y. G. Lin, Y. K. Hsu, C. T. Wu, S. Y. Chen, K. H. Chen and L. C. Chen, *Diamond Relat. Mater.*, 2009, **18**, 433.
2 F. Raimondi, G. G. Scherer, R. Kötz and A. Wokaun, *Angew. Chem., Int. Ed.*, 2005, **44**, 2190.
3 J. C. Frost, *Nature*, 1988, **334**, 577; P. H. Matter, D. J. Braden and U. S. Ozkan, *J. Catal.*, 2004, **223**, 340; I. Kasatkin, P. Kurr, B. Kniep, A. Trunschke and R. Schlögl, *Angew. Chem., Int. Ed.*, 2007, **46**, 7324; B. Frank, F. C. Jentoft, H. Soerijanto, J. Kröhnert, R. Schlögl and R. Schomäcker, *J. Catal.*, 2007, **246**, 177; D. R. Palo, *Chem. Rev.*, 2007, **107**, 3992; Y. K. Lin, Y. H. Su, Y. H. Huang, C. J. Hsu, Y. K. Hsu, Y. G. Lin, K. H. Huang, S. Y. Chen, K. H. Chen and L. C. Chen, *J. Mater. Chem.*, 2009, **19**, 9186; Y. G. Lin, Y. K. Hsu, S. Y. Chen, L. C. Chen and K. H. Chen, *J. Mater. Chem.*, 2010, DOI: 10.1039/c0jm02605k.
4 B. L. Kniep, F. Girgsdies and T. Ressler, *J. Catal.*, 2005, **236**, 34.
5 Y. G. Lin, Y. K. Hsu, S. Y. Chen, Y. K. Lin, L. C. Chen and K. H. Chen, *Angew. Chem., Int. Ed.*, 2009, **48**, 7586.
6 B. L. Hayes, *Microwave Synthesis: Chemistry at the Speed of Light*, CEM Publishing, Matthews, NC, 2003; C. O. Kappe, *Angew. Chem., Int. Ed.*, 2004, **43**, 6250; T. A. Nissinen, Y. Kiros, M. Gasik and M. Leskelä, *Chem. Mater.*, 2003, **15**, 4974; D. D. Young, J. Nichols, R. M. Kelly and A. Deiters, *J. Am. Chem. Soc.*, 2008, **130**, 10048.
7 C. J. Ko, Y. K. Lin and F. C. Chen, *Adv. Mater.*, 2007, **19**, 3520.
8 Y. Li, B. Tan and Y. Wu, *Chem. Mater.*, 2008, **20**, 567.
9 N. Ashkenov, B. N. Mbenkum, C. Bundesmann, V. Riede, M. Lorenz, D. Spemann, E. M. Kaidashev, A. Kasic, M. Schubert, M. Grundmann, G. Wagner, H. Neumann, V. Darakchieva, H. Arwin and B. Monemar, *J. Appl. Phys.*, 2003, **93**, 126; T. Yu, X. Zhao, Z. X. Shen, Y. H. Wu and W. H. Su, *J. Cryst. Growth*, 2004, **268**, 590.
10 L. Seyfried, F. Garin, G. Maire, J. M. Thiebaut and G. Roussy, *J. Catal.*, 1994, **148**, 281.
11 K. J. Rao, B. Vaidhyanathan, M. Ganguli and P. A. Ramakrishinan, *Chem. Mater.*, 1999, **11**, 882.

